

# The Chemical and Physical Properties of Electrochemically Prepared Polyaniline Hexafluorophosphate (PAPF<sub>6</sub>)

KYUNG MOON CHOI and KEU HONG KIM\*

Department of Chemistry, Yonsei University, Seoul 120, Korea

## SYNOPSIS

Polyaniline hexafluorophosphate (PAPF<sub>6</sub>) was synthesized by electrochemical oxidation from 0.2 M aniline in acetonitrile solution containing 0.1 M TEAPF<sub>6</sub> as the supporting electrolyte. From polarographic and cyclic voltammetry results, the values of the half-wave potential ( $E_{1/2}$ ) and  $\alpha n$  were calculated to be 774 mV and 0.589, respectively. The morphology of the PAPF<sub>6</sub> sample was determined from SEM. Thermal analyses for PAPF<sub>6</sub> and other polyaniline-based systems show distinguishable, thermal characteristics depending on the doping methods for the anions. Also, the maximum values ( $R_{max}$ ) of the reaction rates ( $R$ ) for these polymers were obtained. The electrical conductivity of the PAPF<sub>6</sub> pellet was measured at temperatures from -170 to 25°C. From a plot of conductivity vs.  $1/T$ , an activation energy ( $E_a$ ) of 0.057 eV was obtained. The conduction mechanism in the pressed pellet of PAPF<sub>6</sub> is suggested to be hopping conduction. The various ESR-parameters were obtained from the ESR curve at room temperature.

## INTRODUCTION

Organic conducting polymers have attracted attention not only from the scientific viewpoint, but also because of the extensive possible applications, such as in solar batteries,<sup>1</sup> rechargeable batteries,<sup>2</sup> electronic switching elements,<sup>3</sup> electro-optic devices,<sup>4</sup> radiation detectors,<sup>5</sup> and sensors.<sup>6</sup> Recently, the trend in the studies of conducting polymers has been toward research on electrochemically synthesized conducting polymers. Diaz<sup>7</sup> synthesized the so-called "pyrrole blacks," obtained by electro-oxidation of pyrrole in acetonitrile containing various supporting electrolytes.

Various methods for the electro-oxidation of poly(*p*-phenylene) films from benzene or biphenyl have also been proposed.<sup>8</sup> Recent reports<sup>9,10</sup> for electrochemically prepared polyaniline encouraged us to investigate the aniline systems. Polyaniline is a useful conducting polymer from the practical point of view for the following reasons: (1) Polyaniline is electrochemically reversible. Thus, since there is no

discrimination between the anodic oxidation and cathodic reduction reactions, polyaniline is a reasonable electrode material for rechargeable batteries. (2) Sample preparation by both chemical and electrochemical methods is possible; thus, the reaction conditions for polymerization are not fastidious. What is more, the conducting forms obtained by these two methods are stable in air and water. (3) Chemical durability against air oxidation and moisture is high enough so that no special precautions for handling are necessary.

Jozefowicz et al.<sup>11</sup> found that the open circuit potential for a pressed pellet of polyaniline, placed between a mercury electrode and an aqueous H<sub>2</sub>SO<sub>4</sub> solution, decreases with an increase in the pH of the solution. This was explained in terms of the polyaniline pellet having both ionic and electronic conductivity. Also, ESR<sup>12</sup> and NMR<sup>13</sup> studies of polyaniline-based conducting polymers have been reported recently. MacDiarmid et al.<sup>14</sup> reported on the utility of polyaniline as a cathode-active material in rechargeable batteries with aqueous and non-aqueous electrolytes, and in electrochromic displays. The specific weight is much lower than that of inorganic conductors. Sariciftci et al.<sup>15</sup> proposed that polyaniline has potential in applications such as for

\* To whom correspondence should be addressed.

switching material or electrochromic displays. As for the color change in metal and insulator, this can be influenced by the formation of electronic states, such as solitons, polarons, and bipolarons in polymers.

Polyaniline is unusual among macromolecular systems; unlike most conducting polymers it exhibits a proton doping mechanism, in addition to the electrochemical doping process, involving counter ion intercalation on oxidation. By electrochemical oxidation or reduction, various anions or cations are doped in polyaniline-based conducting polymers, thus, transferring them into a highly conducting metallic state without any gap in the electronic band structure. Polyaniline-based systems, doped with anions or cations, have generally been studied as films. A study is needed that will cover conditions found in practical applications, such as the properties of pelletized polyaniline samples. Thus, in this work we obtained the results of electrochemical studies, morphology, ESR measurements, and thermal stability for hexafluorophosphate-doped polyaniline (PAPF<sub>6</sub>), and suggest the conduction mechanism in pellets.

## EXPERIMENTAL

### Materials

As the supporting electrolytes, tetraethylammonium *p*-toluenesulfonate (TEATS), tetraethylammonium tetrafluoroborate (TEABF<sub>4</sub>), tetraethylammonium perchlorate (TEAP), and tetraethylammonium hexafluorophosphate (TEAPF<sub>6</sub>) were employed. These materials were obtained from the Aldrich Chemical Co. Ferric perchlorate, Fe(ClO<sub>4</sub>)<sub>3</sub>, a strong oxidant, was obtained from the Fluka Chemical Co. Before use, materials were dried in a vacuum oven at 25°C for two days. Acetonitrile was purified by vacuum distillation and the solvent was passed through a column packed with alumina and trifluoroacetic anhydride for the removal of water. The alumina treatment was followed by distillation from calcium hydride to obtain the highest purity material.

### Sample Preparation

#### *Electrochemically Prepared Sample*

A three-electrode cell was equipped with Pt working and counter electrodes and a saturated calomel electrode (SCE) as a reference electrode. The working and counter electrodes were 2 cm<sup>2</sup> Pt plates.

Polyaniline hexafluorophosphate (PAPF<sub>6</sub>) was electrochemically synthesized from 0.2 M aniline in acetonitrile (AN) solution containing 0.1 M TEAPF<sub>6</sub> as the supporting electrolyte. For the removal of dissolved oxygen, a nitrogen stream was passed through the solution in the reaction cell for 30 min before each experiment. The temperature of the solution in the cell was maintained at 25°C using a circulator (Lauda Co.). An external voltage of 2 V vs. SCE was supplied at the anode electrode for electrochemical polymerization.

Polyaniline *p*-toluenesulfonate (PATS), polyaniline tetrafluoroborate (PABF<sub>4</sub>) and polyaniline perchlorate (PAP:Ele.) were prepared from 0.2 M aniline in AN solutions containing 0.1 M TEATS, TEABF<sub>4</sub>, or TEAP, using a potential of 1.5, 1.8, or 2 V vs. SCE, respectively.

The anodic precipitates produced from the electrochemical reactions remained on the electrode as insoluble materials, and they were confirmed to be the electrically conductive polymers. These products were removed from the anode electrode, rinsed with acetonitrile, and dried in a vacuum oven for 2 days until constant weight was achieved.

#### *Chemically Prepared Sample*

Polymerization of the aniline was performed in water using a strong oxidant, Fe(ClO<sub>4</sub>)<sub>3</sub>. The 0.3 M aniline and 0.7 M Fe(ClO<sub>4</sub>)<sub>3</sub> solutions were prepared in aqueous conditions. The solutions were simultaneously cooled down to 0°C, and the dissolved oxygen in the solutions was removed by nitrogen bubbling for at least 30 min. When these solutions were mixed, black precipitates immediately appeared. The mixed solution was kept at 0°C under nitrogen bubbling and continuous stirring for 2 h. The precipitates obtained from this mixed solution were washed with distilled water and dried in vacuum. Polyaniline perchlorate (PAP:Chem.) thus obtained is a black conducting powder, which is stable in its oxidized state in air.

### Elemental Analysis

Elemental analyses for PAPF<sub>6</sub>, PATS, PABF<sub>4</sub>, PAP (Ele.), and PAP (Chem.) were performed to determine the dopant contents by using an elemental analyzer (Perkin Elmer, Model No. 240 C). The results are shown in Table I.

### Electrochemical Measurements

The electrochemical syntheses, polarography, and cyclic voltammetry measurements were carried out

**Table I** Elemental Analysis for Various Polyaniline-Based Polymers

Polyaniline Derivatives	Polymer Chains (%)			Dopant (%)
	C	H	N	
PATS	37.90	2.99	7.80	51.29
PABF <sub>4</sub>	51.00	4.10	9.93	34.97
PAPF <sub>6</sub>	56.67	5.68	10.51	27.14
PAP (Ele.)	62.88	5.56	11.19	20.37
PAP (Chem.)	35.11	3.08	6.92	54.89

with a potentiostat (Tacussel, Polaropulse type PRG-5), with the potential sweeps applied from a function generator (Tacussel, Model No. GSTP 3). The polarogram and cyclic voltammogram were obtained by using a polarography recorder (Tacussel, Type EPL 1) and an X-Y recorder (Rikadenki, Model No. RW-11 T), respectively. A specially designed cell was used, and purified nitrogen was bubbled before each electrolysis, to eliminate oxygen. The solution was stirred with a magnetic stirring bar. The Pt counter and working electrodes were precleaned and conditioned by potential pulsing between the hydrogen and oxygen evolution regions. This procedure results in the formation of an electrode surface with reproducible electrochemical behavior.

### Conductivity Measurements

The PAPF<sub>6</sub> for conductivity measurements was obtained from aniline using a potential of 2 V and a synthesis time of 10 h. The anodic insoluble precipitates were rinsed with AN and dried in a vacuum at 25°C. The conducting polymer was obtained as a fine powder, which was subjected to a pressure of 98.06 MPa, and as a disc-shaped pellet, which was 13 mm in diameter and 2.8 mm in thickness. The conductivity of the pressed pellet of PAPF<sub>6</sub> was measured using Pt-wires as probes at temperatures from -170 to 25°C. The current and the voltage were measured by a digital electrometer (Keithley, Model No. 616) and a digital multimeter (Keithley, Model No. 642), respectively. The specimen was in a temperature-controlled chamber and the temperatures at measurement were checked using a digital thermometer (Seoul Control Co., SR-6200, Model No. G-116). The conductivity was measured while raising the temperature at a heating rate of 1°C/min, and the conductivity values were computed directly from the measured resistance and sample dimensions.

### ESR Measurements

Electron spin resonance (ESR) measurements were carried out with a EPR Spectrometer (Bruker, Model No. ER 200 E-SRC). PAPF<sub>6</sub> powders were placed in the ESR tube at 25°C, and the ESR spectrum of PAPF<sub>6</sub> in Figure 12 was obtained under the following conditions: (Scan range, 100 G; Microwave frequency, 9.45 GHz; Microwave power, 20 dB, 2 mW; Modulation frequency, 100 KHz; Modulation time constant, 200 ms; Modulation amplitude, 4 G; Receiver gain,  $2.5 \times 10^3$ ).

### Thermal Analysis

Thermal analyses of the polyaniline-based conducting polymers, PAPF<sub>6</sub>, PATS, PABF<sub>4</sub>, and PAP, were performed using a thermal analyzer (Rigaku, Model No. 8150). Thermogravimetry (TGA) curves in a nitrogen atmosphere were obtained at temperatures in the range of 25–800°C with a heating rate of 10°C/min.

### Scanning Electron Microscope (SEM)

An external potential of 2 V was continuously applied to an acetonitrile solution containing 0.2 M aniline and 0.1 M TEAPF<sub>6</sub> for 10 h; a PAPF<sub>6</sub> film was thus formed on the anode electrode. By using an ion coater (Eiko, Model No. IB-3), gold was deposited on the surface of the electrode coated with the PAPF<sub>6</sub> film. SEM measurements of the sample film were made using a scanning electron microscope (Hitachi, Model No. S-510).

## RESULTS AND DISCUSSION

### Polarography

Most quantitative analyses in polarography deal with the proportionality between the diffusion-limited current ( $id$ ) and bulk concentration ( $Co^*$ ) as expressed in the Ilkovic equation. The value of  $id$  is the current that flows during a single lifetime when the DME is held at some potential in the mass transfer-controlled region for electrolysis, and it is considered to be the convective movement between the electrode and solution during drop growth. The half-wave potential,  $E_{1/2}$ , is defined as the potential at the mid-point of the polarographic wave where  $i = id/2$ . The value of  $E_{1/2}$  is sensitively dependent on the presence of different complexing species, including supporting electrolyte anions, and is used for "fingerprinting," but with extreme caution.

In the sampled-current voltammetric experiment, the relationship between currents and the corresponding potentials for a reversible reaction is expressed in eq. (1):

$$E = E_{\frac{1}{2}} + (2.303 RT/nF) \log[(id - i)/i], \quad (1)$$

where  $n$  is the number of electrons transferred in the reversible reaction, and  $E_{\frac{1}{2}}$  is the half-wave potential. From eq. (1) it is seen that the values of  $E_{\frac{1}{2}}$  and  $n$  can be obtained from the  $y$ -intercept and the slope of a plot of  $E$  vs.  $\log[(id - i)/i]$  for a polarographic wave, respectively, and the reversibility can be predicted from the "wave slopes." A quicker test for reversibility is to see if  $|E_{\frac{3}{4}} - E_{\frac{1}{4}}| = 56.4/n$  (mV) at 25°C. The potentials of  $E_{\frac{3}{4}}$  and  $E_{\frac{1}{4}}$  are those for which  $i = \frac{3}{4}id$  and  $i = \frac{1}{4}id$ , respectively.

On the other hand, in the case of an irreversible reaction, it must be considered that the wave has less than the theoretical slope for the number of electrons transferred. Thus, eq. (1) can be modified using a transfer coefficient,  $\alpha$ . The relationship between current and corresponding potential for an irreversible couple is expressed by eq. (2):

$$E = E_{\frac{1}{2}} + (2.303 RT/\alpha nF) \log[(id - i)/i]. \quad (2)$$

For the case of irreversible reactions, the kinetic parameters ( $\alpha$ ,  $k$ ,  $n$ ) can be computed. That is, we can obtain the values of  $\alpha n$  and  $E_{\frac{1}{2}}$  from a plot of  $E$  vs.  $\log[(id - i)/i]$ .

A polarogram of the 0.2 M aniline in AN solution containing 0.1 M TEAPF<sub>6</sub> was obtained at 25°C. A plot of  $E$  vs.  $\log[(id - i)/i]$  obtained from this po-

larographic wave is shown in Figure 1. The value of  $E_{\frac{1}{2}}$  obtained from the  $y$ -intercept of Figure 1 is 774 mV and the value of  $\alpha n$  calculated from the slope is 0.589. In general systems, the magnitude of  $\alpha$  turns out to lie between 0.3 and 0.7, and it can usually be approximated by 0.5 in the absence of actual measurements. From the  $\alpha n$ -value of 0.589, it is predicted that the value of the number of electrons transferred in the electrode reaction ( $n$ ) and the transfer coefficient ( $\alpha$ ) may be 1 and 0.589, respectively. Also, the values of  $E_{\frac{1}{4}}$  and  $E_{\frac{3}{4}}$  computed from the polarographic wave are 732.8 and 796.9 mV, respectively; thus the value of  $|E_{\frac{3}{4}} - E_{\frac{1}{4}}|$  is 64.1 mV. Since the value of  $|E_{\frac{3}{4}} - E_{\frac{1}{4}}|$  is 56.4/ $n$  (mV) in the case of a reversible reaction, it is predicted that this electrochemical reaction is irreversible. In order to obtain more supporting evidence for this electrode reaction, cyclic voltammetry analysis was performed.

### Cyclic Voltammetry

A cyclic voltammogram for acetonitrile solution containing 0.2 M aniline and 0.1 M TEAPF<sub>6</sub> was obtained in the potential range from -600 to 1900 mV at 25°C with varying scan rates ( $v$ ). The result is shown in Figure 2. In the cyclic voltammetry analysis, a charging current ( $ic$ ) induced by the continuously changing potential always flows; thus the faradaic current ( $if$ ) must be computed from a base line of the charging current. As the charging current and the peak current ( $ip$ ) are proportional to  $v$  and  $\sqrt{v}$ , respectively, consideration for the proper value of  $|ic|/ip$  as expressed in eq. (3) is important.

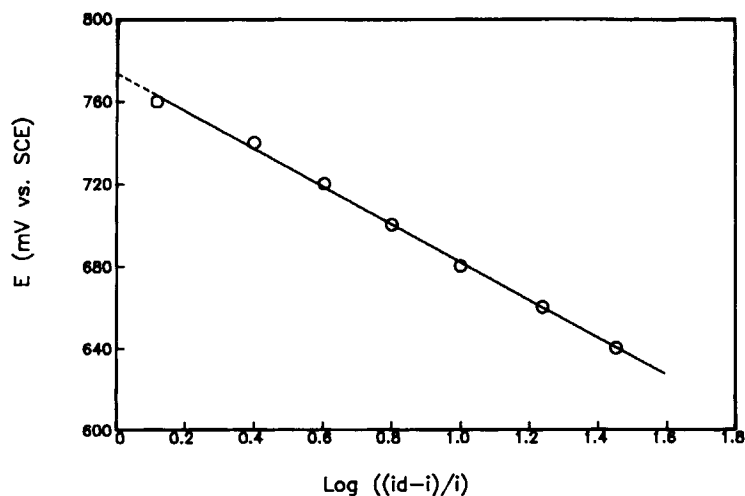


**Figure 1** Plot of  $E$  vs.  $\log[(id - i)/i]$  for 0.2 M aniline in acetonitrile containing 0.1 M TEAPF<sub>6</sub> at 25°C.

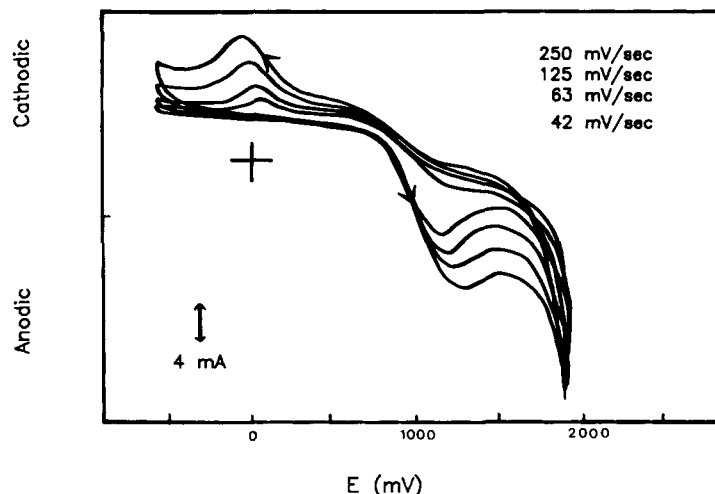


**Figure 2** Cyclic voltammogram of a polyaniline hexafluorophosphate in AN solution at 25°C.

$$\frac{|ic|}{ip} = K \frac{\sqrt{v}}{n^{3/2} \times Co^*} \quad (3)$$

Namely, pertinent selection of the values for the scan rate and bulk concentration was made during the cyclic voltammetry measurements. Figure 2 shows a single cathodic and anodic peak couple.

The changes in anodic and cathodic peak potentials ( $E_{pa}$ ,  $E_{pc}$ ) with scan rate are shown in Figure 3. Generally, the reversibility of an electrochemical reaction can be simply determined from the dependence of peak potential ( $E_p$ ) on scan rate. The peak potentials are not dependent on the scan rate in reversible couples but are dependent on the scan

rate in irreversible couples. Figure 3 shows that the peak potential is a function of scan rate, shifting in the negative (for a reduction:  $E_{pc}$ ) and positive (for an oxidation:  $E_{pa}$ ) directions with increasing scan rates. Therefore, it is clarified that the anodic and cathodic reaction for this system is irreversible. These results, obtained from the cyclic voltammetry analysis, agree with the results predicted by the polarographic results.

#### TGA and DSC Measurements

TGA and DSC measurements for the PAPF<sub>6</sub> and other polyaniline-based conducting polymers (PATS, PABF<sub>4</sub>, and PAP) were performed to obtain

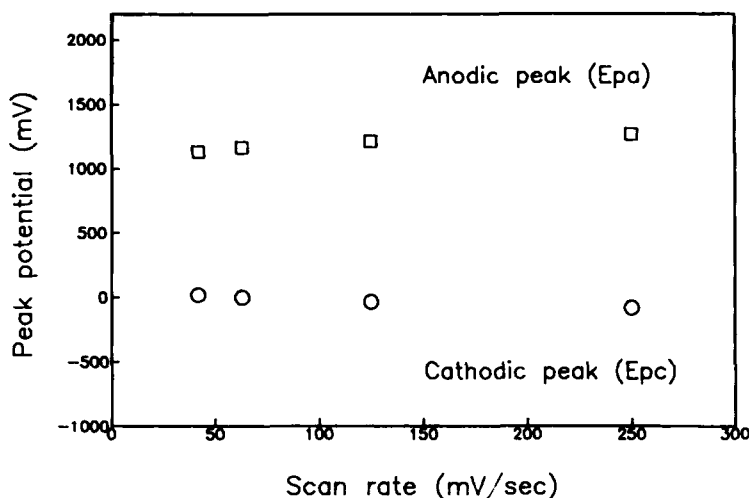


**Figure 3** Variation of anodic and cathodic peak potentials with scan rates for 0.2 M aniline in AN solution containing 0.1 M TEAPF<sub>6</sub> at 25°C.

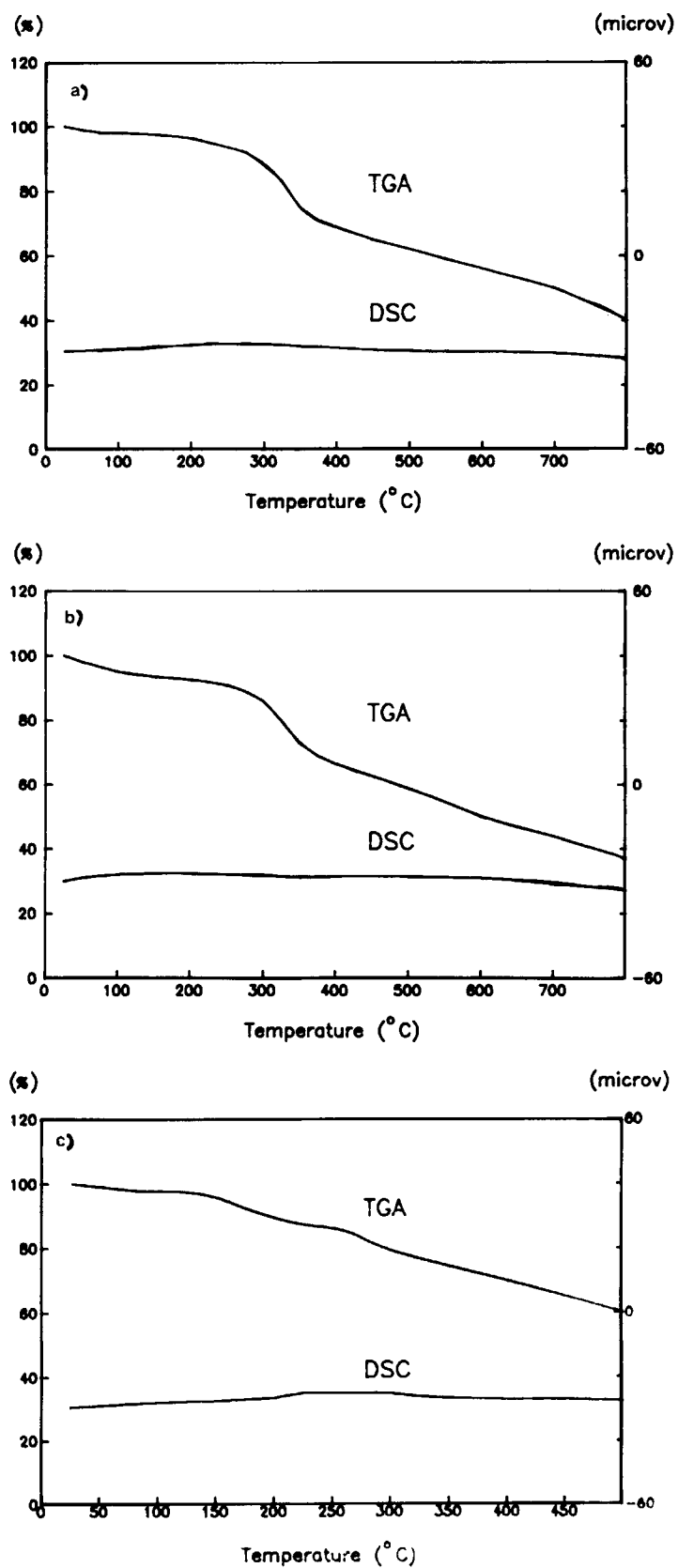


**Figure 4** TGA and DSC curves of (a) PATS, (b) PABF<sub>4</sub>, (c) PAPF<sub>6</sub>, (d) PAP (Chem.), and (e) PAP (Ele.) in nitrogen.

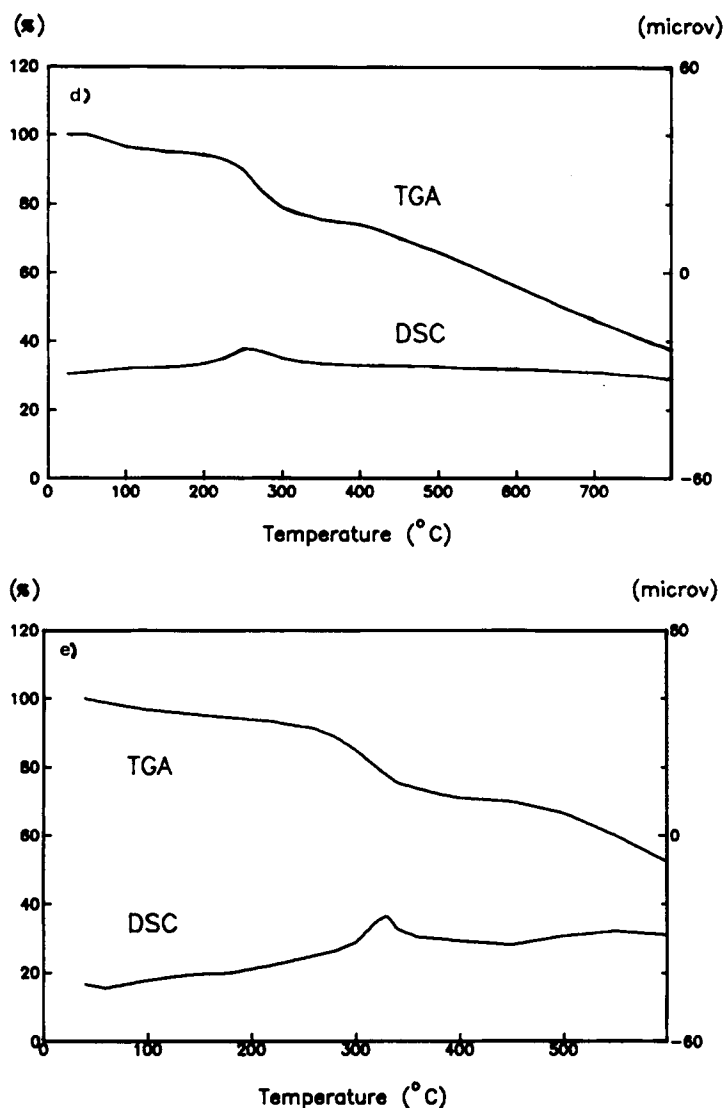
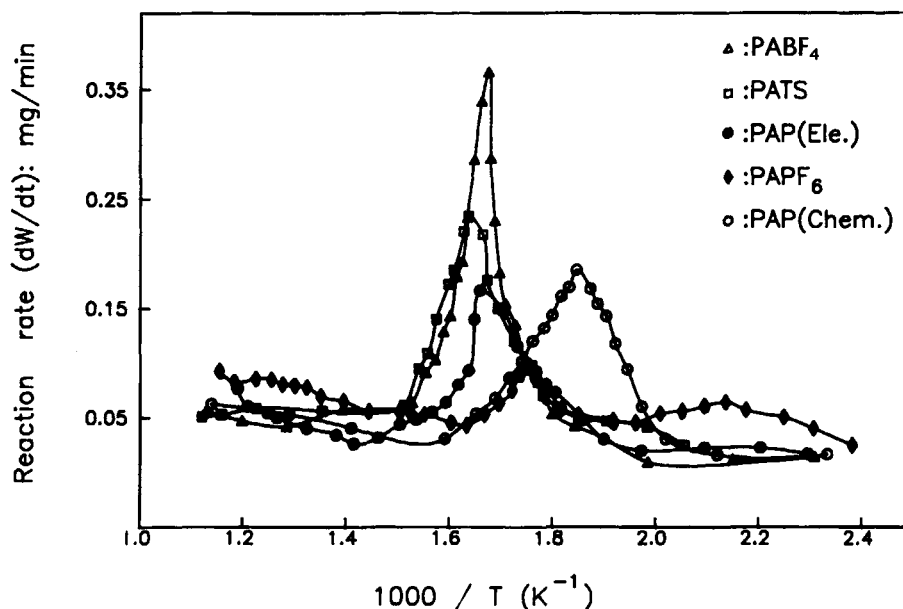


Figure 4 (Continued from the previous page)

information on their thermal characteristics in the temperature range of 25–800°C, and the results are shown in Figure 4. As shown by the TGA curves in Figure 4, most of the weight loss for each sample takes place in a narrow temperature range. The DSC curves, corresponding to the TGA results, were also obtained and are shown in Figure 4. The DSC measurements on systems doped with perchlorate anions, PAP (Ele.) and PAP (Chem.), exhibit exothermic peaks at 330°C and 250°C, respectively. On the other hand, no DSC peaks for the other samples (PAPF<sub>6</sub>, PATS, and PABF<sub>4</sub>) were obtained in the measured temperature range.

The reaction rate ( $R: dW/dt$ ), computed from the TGA results for the polyaniline-based polymers, is plotted against the reciprocal of the absolute tem-

perature in Figure 5. Also, the values of the temperature ( $T_{\max}$ ) and reaction rate ( $R_{\max}$ ) at the maximum peak points of the reaction rate are listed in Table II. Among these samples, the PABF<sub>4</sub>, PATS, PAPF<sub>6</sub>, and PAP (Ele.) samples were prepared by the electrochemical doping of anions, and the PAP (Chem.) sample was obtained by the chemical doping of perchlorate anions. From the data in Figure 5 and Table II, the following results were observed: (1) The temperatures at the beginning and ending points of weight loss for electrochemically obtained polymers are almost the same, whereas the chemically prepared polymer (PAP: Chem.) has a lower beginning temperature for weight loss. (2) The thermal reactions for electrochemically prepared polymers occur abruptly over a narrower



**Figure 5** The temperature dependence of the reaction rates for various polyaniline-based conducting polymers.

temperature range than for the chemical polymer. From these results, it is obvious that the polyaniline-based polymers show distinguishable thermal characteristics, attributable to the different anion-doping methods, such as electrochemical or chemical preparation.

### Scanning Electron Microscopy (SEM)

For the morphology analysis of the PAPF<sub>6</sub> film, a film was coated on the Pt electrode placed in the AN solution, containing 0.2 M aniline and 0.1 M TEAPF<sub>6</sub>, with a potential supply of 2 V vs. SCE. The growth rate of polymer depends on the current density, which is related to factors such as the resistance of the electrolytic solution, concentration of aniline, applied voltage, etc. During the synthesis, the color of the anodic precipitate changed from yellow-brown to dark chestnut, and then almost black.

The morphology of the PAPF<sub>6</sub> film on the Pt plate is shown in Figure 6. As shown in the SEM results, the surface of the PAPF<sub>6</sub> film shows a bark pattern, oriented as regular grains in wood, and material similar to netting thread design crusted on the film.

### Conductivity

Conducting polymers are easily reduced and oxidized by chemical and electrochemical doping methods,

and the electrical conductivity of these polymers depends on various factors, such as the concentration and species of dopants, the nature and structure of the polymer arrays, the morphology, the orientation of the conducting species, the applied voltage, the pressure, the film density, the employed solvent, etc. It has been reported that in the case of the best conducting organic polymers, the oxidized- or doped-conducting polymers behaved similar to metallic conductors, whereas the reduced or neutral undoped systems had insulating or semiconductor-like characteristics.<sup>16</sup>

Various models and equations to explain the electrical conduction mechanisms in conducting organic polymers have been suggested in previous reports.<sup>17-22</sup> No detailed and reasonable conduction mechanism has yet been proposed, however, that can fully explain the polymeric system; the unilateral application of band structure of these amorphous

**Table II** TGA Results for Polyaniline-Based Conducting Polymers

Polyaniline Derivatives	$R_{\max}$ (mg/min) at $T_{\max}$
PABF <sub>4</sub>	0.366 (at 324°C)
PATS	0.234 (at 338°C)
PAP (Ele.)	0.166 (at 327°C)
PAPF <sub>6</sub>	0.092 (at 300°C)
PAP (Chem.)	0.185 (at 269°C)



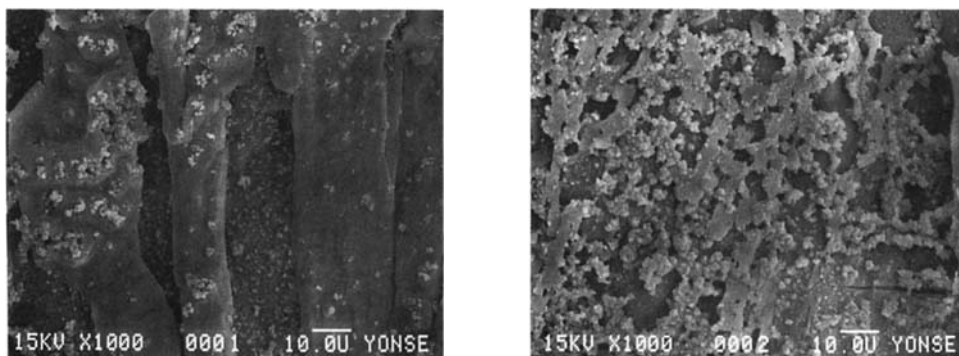


**Figure 6** Scanning electron micrographs of a polyaniline hexafluorophosphate.

matrices is also unreasonable. Thus, the suggestion of a conduction mechanism for polymeric organic conductors needs to be considered. The conduction mechanism in a pressed pellet of PAPF<sub>6</sub> is suggested, employing eqs. (4)–(7).

The conductivity as a function of temperature for hopping transport of electrons between localized sites has been found to conform to the  $\exp(-\text{const}/T^\alpha)$  form observed in amorphous semiconductors ( $\alpha = \frac{1}{4}$ ) by Mott<sup>17</sup> and to sputtered granular metal films ( $\alpha = \frac{1}{2}$ ) by Sheng.<sup>18</sup> But, as this relationship is based on the assumption that the concentration of charge carriers is not affected by temperature, the actual application to semiconductors may not be precise. Also, following Greaves,<sup>19</sup> a variable range hopping conduction is given in eq. (4):

$$\sigma T^{1/2} = \exp[-(B/T^{1/4})], \quad (4)$$

where  $B$  is a constant. On the other hand, electronic

conduction including the grain boundary potential is given by Matare's equation,<sup>20</sup>

$$\sigma = AT^{1/2} \exp(-Ea/kT), \quad (5)$$

where  $A$  is a constant related to the electric field strength and effective mass of electrons, and  $Ea$  is the height of the potential barrier. Also, Zeller<sup>21</sup> and Orton<sup>22</sup> have shown that tunneling and thermionic emission conduction are given by eqs. (6) and (7), respectively:

$$\sigma = \sigma_0 \exp(-A'T^{-1/2}) \quad (6)$$

and

$$\sigma = \sigma_0 T^{-1/2} \exp(-Ea/kT). \quad (7)$$

The electrical conductivity for the pressed pellet of PAPF<sub>6</sub> was measured by a four-probe technique

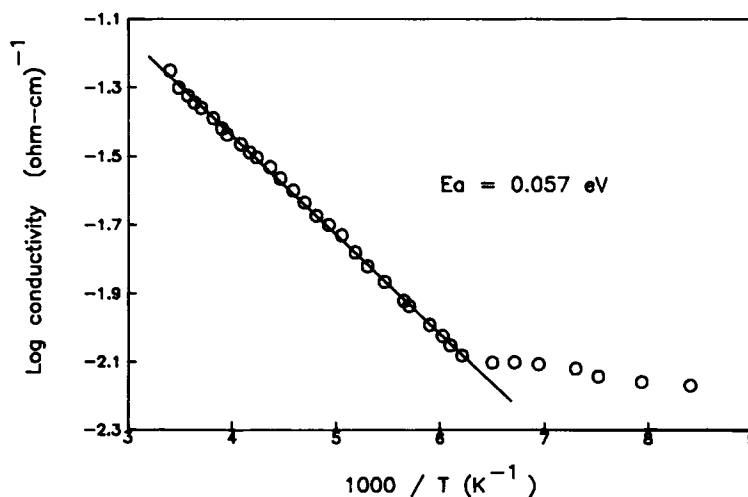


**Figure 7** The electrical conductivity as a function of temperature for a polyaniline hexafluorophosphate.

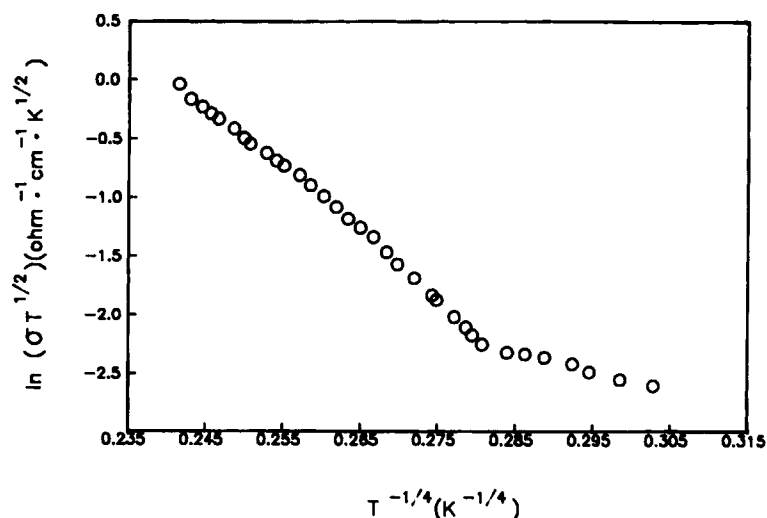


**Figure 8** The temperature dependence of the electrical conductivity for polyaniline hexafluorophosphate based on the hopping conduction mechanism.

at temperatures from  $-170$  to  $25^{\circ}\text{C}$  under a low applied field to ensure Ohmic behavior. Figure 7 shows the temperature dependence of the conductivity for the  $\text{PAPF}_6$  pellet. The conductivity increases linearly with increasing temperature, satisfying the Arrhenius equation,  $\sigma = \sigma_0 \exp(-Ea/kT)$ . The values of  $Ea$  and  $\log \sigma$  at  $25^{\circ}\text{C}$  were obtained from the slope and straight line in Figure 7 and were  $0.057$  eV and  $-1.25$   $(\text{ohm}\cdot\text{cm})^{-1}$ , respectively. The temperature dependencies of the electrical conductivity of the  $\text{PAPF}_6$  pellet, based on eqs. (4) through (6), for the hopping, electronic (including the grain boundary potential), and tunneling conduction mechanisms are shown in Figures 8–10, respectively. A plot based

on eq. (7) was excluded due to its poor linearity. Figures 8 and 9, obtained from the hopping and electronic (including grain boundary potential) conduction mechanisms, show linearities, whereas Figure 10 shows more deviation from linearity than do Figures 8 and 9. Thus, it is suggested that the conduction mechanism in the pressed pellet of  $\text{PAPF}_6$  is the hopping conduction, and the conductivity increases with  $\text{PF}_6^-$  anion doping as it serves as an electron acceptor.

#### ESR Measurements

A number of ESR studies<sup>23–25</sup> for conducting polymers, especially polypyrrole-based systems, have

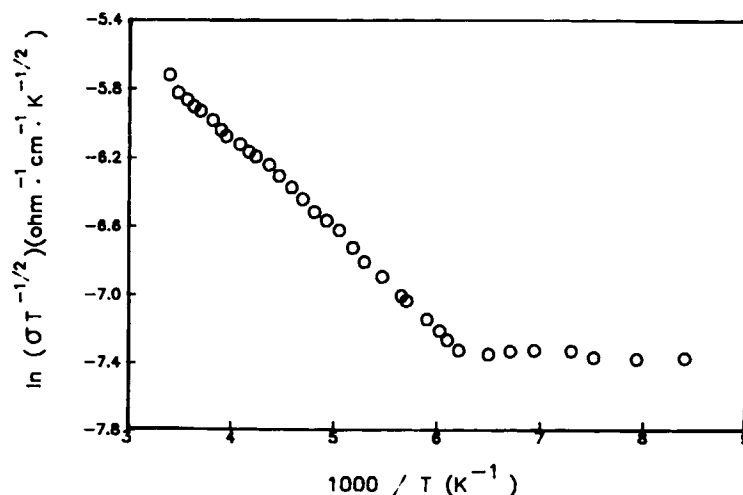


**Figure 9** The temperature dependence of the electrical conductivity for polyaniline hexafluorophosphate based on  $\sigma = AT^{1/2} \exp(-Ea/kT)$ .

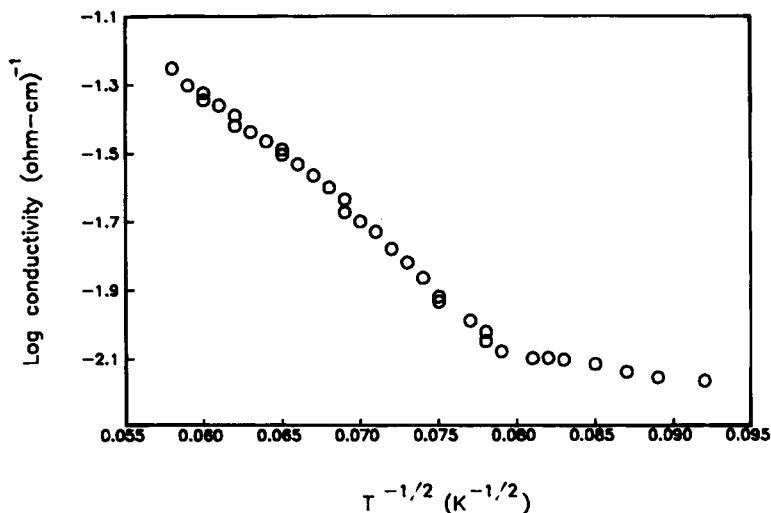


**Figure 10** The temperature dependence of electrical conductivity for polyaniline hexafluorophosphate based on the tunneling conduction mechanism.

been reported, which provide structural evidence for polymers and clarify the conduction mechanisms. Also, there have been many efforts to consider the relationships between the parameters of ESR spec-

tra and the transport or electrical properties in conducting polymers. For example, the relationship between the *g*-values, peak-to-peak linewidth ( $\Delta H_{pp}$ ) in the first-derivative spectrum, width at half-height

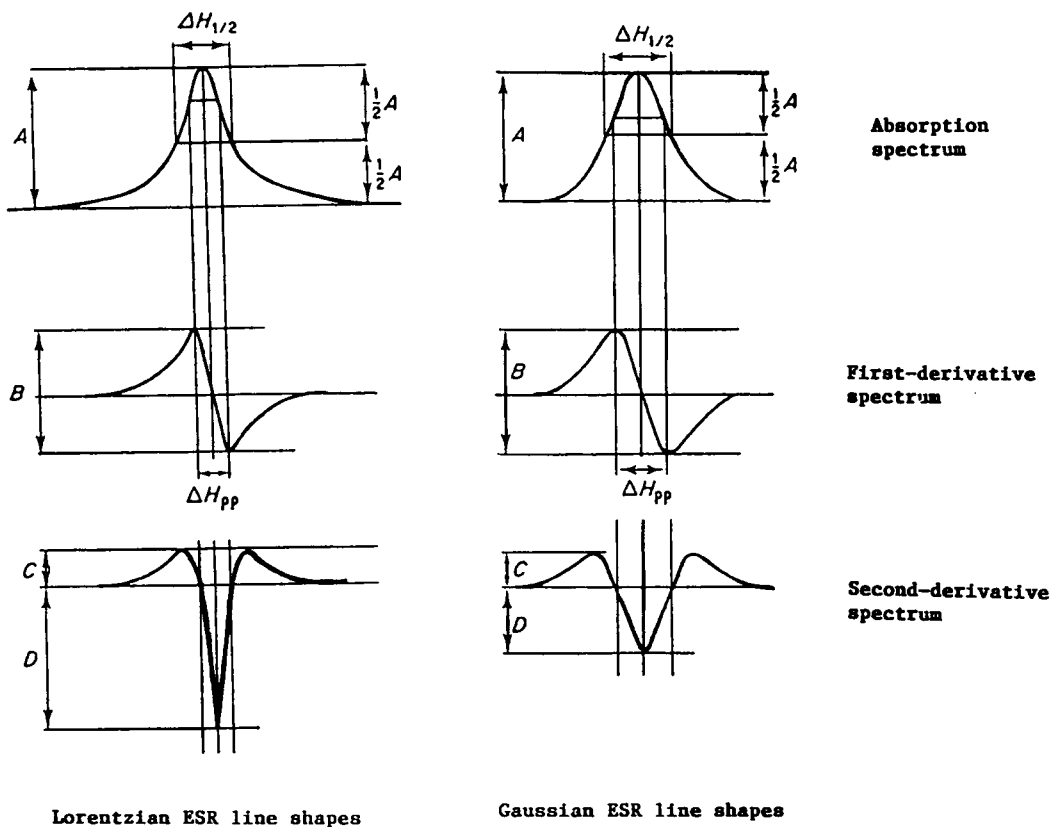


**Figure 11** Lorentzian and Gaussian line shapes for ESR spectra.<sup>26</sup>

**Table III** The Important Measurable Parameters Characterizing Lorentzian and Gaussian Lines<sup>26</sup>

Parameter	Lorentzian Line	Gaussian Line
Width at half-height	$\Delta H_{1/2}$	$\Delta H_{1/2}$
Peak-to-peak width	$\Delta H_{pp} = \frac{H_{1/2}}{\sqrt{3}}$	$\Delta H_{pp} = \left(\frac{2}{\ln 2}\right)^{1/2} \frac{\Delta H_{1/2}}{2}$
Peak amplitude	$A = \frac{2}{\pi \Delta H_{1/2}}$	$A = \left(\frac{\ln 2}{\pi}\right)^{1/2} \frac{2}{\Delta H_{1/2}}$
Peak-to-peak amplitude	$B = \frac{3\sqrt{3}}{\pi} \frac{1}{(\Delta H_{1/2})^2}$	$B = \left(\frac{2}{\pi e}\right)^{1/2} \frac{2 \ln 2}{(\Delta H_{1/2})^2}$
Peak amplitude of positive lobe	$C = A \left(\frac{2}{\Delta H_{1/2}}\right)$	$C = A \left(\frac{16e^{3/2} \ln 2}{(\Delta H_{1/2})^2}\right)$
Peak amplitude of negative lobe	$D = -A \left(\frac{8}{\Delta H_{1/2}}\right)$	$D = -A \left(\frac{8 \ln 2}{\Delta H_{1/2}}\right)$

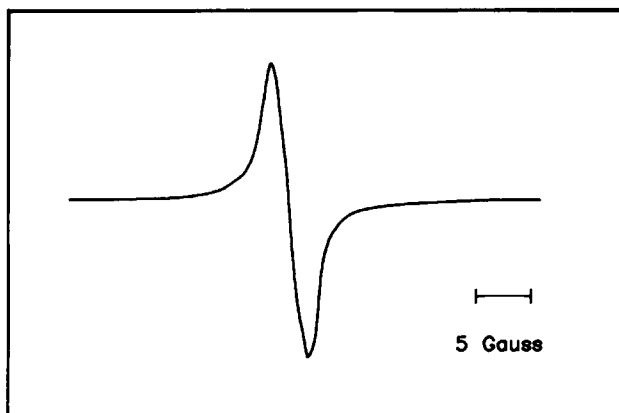
( $\Delta H_{1/2}$ ) in the absorption spectrum, and ratios between peak-heights and the conductivity can be considered, as referenced in Figure 11 and Table III.<sup>26</sup>

Figure 12 shows an ESR peak for PAPF<sub>6</sub> powder at 25°C; the shape is a Gaussian curve, but slightly narrower. The measured values of  $\Delta H_{pp}$  and the  $g$ -factor are 3 Gauss and 2.00578, respectively. On the one hand, correlations between various ESR parameters and transport mechanisms and structural information in polypyrrole-based systems have been carefully interpreted.<sup>23</sup> These reported results for the polypyrrole systems are useful in this work, but more studies and information are necessary to obtain the relationships for these polyaniline-based polymers.

## CONCLUSIONS

From the electrochemical measurements (polarography and cyclic voltammetry), the electrode reaction related to the anodic polymerization is an irreversible reaction and the values of  $E_{1/2}$  and  $\alpha n$ , are obtained at 774 mV and 0.589, respectively. The PF<sub>6</sub><sup>-</sup> anions, which play a role in the initiation of polymerization, are electrochemically doped and form the polaron states along the polyaniline chains as an electron acceptor.

From the electrical conductivity results, the value of  $E_a$  is obtained to be 0.057 eV, and the hopping conduction mechanism is suggested. Also, a single ESR curve for PAPF<sub>6</sub> powder was obtained. From the conductivity and ESR results it can be proposed



**Figure 12** ESR spectrum of polyaniline hexafluorophosphate at 25°C (microwave frequency: 9.45 GHz).

that polaron states are formed along the polymer chains adding to the oxidative doping injection of electron acceptors. Thus, the observed electrical conductivity is due to polarons as charge carriers that hop from state to state.

The financial support of Yonsei University and the partial support of the Korea Research Center for Theoretical Physics and Chemistry are greatly appreciated. We are thankful to Professors H. S. So and J. W. Park for ESR and electrochemical measurements, respectively.

## REFERENCES

1. S. C. Chen, A. J. Heeger, Z. Kiss, and A. G. MacDiarmid, *Appl. Phys. Lett.*, **36**, 1 (1980).
2. P. J. Nigrey, D. MacInnes, D. P. Nairns, A. G. MacDiarmid, and A. J. Heeger, *J. Electrochem. Soc.*, **128**, 1651 (1981).
3. K. Yoshino, S. Ura, S. Sasa, K. Kaneto, and Y. Inuishi, *Jpn. J. Appl. Phys.*, **21**, L507 (1982).
4. K. Yoshino, K. Kaneto, and Y. Inuishi, *Jpn. J. Appl. Phys.*, **22**, L157 (1983).
5. K. Yoshino, S. Hayashi, Y. Kohno, K. Kaneto, J. Okube, and T. Moriya, *Jpn. J. Appl. Phys.*, **23**, L189 (1984).
6. T. Osawa, K. Kaneto, and K. Yoshino, *Jpn. J. Appl. Phys.*, submitted.
7. A. F. Diaz, K. K. Kanazawa, and G. P. Gardini, *J. Chem. Soc. Chem. Commun.*, 635 (1979).
8. S. Aeiayach, J. E. Dubois, and P. C. Lacaze, *J. Chem. Soc. Chem. Commun.*, 1668 (1986).
9. A. F. Diaz and J. A. Logan, *J. Electroanal. Chem.*, **111**, 111 (1980).
10. W. S. Huang, B. D. Humphrey, and A. G. MacDiarmid, *J. Chem. Soc.*, **82**, 2385 (1986).
11. M. Jozefowicz, L. T. Yu, J. Perichon, and R. Buvet, *J. Polym. Sci.*, **22**(C), 1187 (1969).
12. K. Masanori, K. Akira, and S. Kazuo, *Chem. Lett.*, 147 (1986).
13. S. Kaplan, E. M. Conwell, A. F. Richter, and A. G. MacDiarmid, *J. Am. Chem. Soc.*, **110**, 7647 (1988).
14. N. L. D. Somasiri and A. G. MacDiarmid, *J. Appl. Electrochem.*, **18**, 92 (1988).
15. N. S. Sariciftci, H. Kuzmany, and H. Neugebauer, *J. Mole. Elec.*, **3**, 141 (1987).
16. A. J. Frank, S. Glenis, and A. J. Nelson, *J. Phys. Chem.*, **93**, 3818 (1989).
17. N. F. Mott, *Philos. Mag.*, **19**, 835 (1969); V. Ambegaokar, B. I. Halperin, and J. S. Langer, *Phys. Rev. B*, **4**, 2612 (1971).
18. P. Sheng, B. Abeles, and Y. Arie, *Phys. Rev. Lett.*, **31**, 44 (1973).
19. G. N. Greaves, *J. Non-Cryst. Solids*, **11**, 427 (1973).
20. M. F. Mataré, *J. Appl. Phys.*, **56**, 2605 (1984).
21. H. R. Zeller, *Phys. Rev. Lett.*, **28**, 1452 (1972).
22. J. W. Orton and M. Powell, *J. Rep. Prog. Phys.*, **43**, 1263 (1980).
23. J. C. Scott, P. Pflugger, M. T. Krounbi, and G. B. Street, *Phys. Rev. B*, **28**(4), 2140 (1983).
24. T. C. Chung, A. Feldblum, A. J. Heeger, and A. G. MacDiarmid, *J. Chem. Phys.*, **74**(10), 5504 (1981).
25. J. L. Brédas, B. Thémans, and J. M. André, *Am. Phys. Soc.*, **27**(12), 7827 (1983).
26. J. F. Rabek, *Experimental Methods in Polymer Chemistry*, Wiley, New York, 1980, p. 332.

Received January 28, 1991

Accepted March 20, 1991